Osteoporos Int (2016) 27:1493–1505
DOI 10.1007/s00198-015-3381-x

ORIGINAL ARTICLE

Glucocorticoids impair bone formation of bone marrow stromal stem cells by reciprocally regulating microRNA-34a-5p

H. Kang[1] · H. Chen[1] · P. Huang[1] · J. Qi[1] · N. Qian[1] · L. Deng[1,2] · L. Guo[1,2]

Received: 4 August 2015 / Accepted: 20 October 2015 / Published online: 10 November 2015

Abstract
Summary The inhibitory effects of glucocorticoids (GCs) on bone marrow stromal stem cell (BMSC) proliferation and osteoblastic differentiation are an important pathway through which GCs decrease bone formation. We found that microRNA-34a-5p was a critical player in dexamethasone (Dex)-inhibited BMSC proliferation and osteogenic differentiation. MicroRNA-34a-5p might be used as a therapeutic target for GC-impaired bone formation.
Introduction The inhibitory effects of glucocorticoids (GCs) on bone marrow stromal stem cell (BMSC) proliferation and osteoblastic differentiation are an important pathway through which GCs decrease bone formation. The mechanisms of this process are still not completely understood. Recent studies implicated an important role of microRNAs in GC-mediated responses in various cellular processes, including cell proliferation and differentiation. Therefore, we hypothesized that these regulatory molecules might be implicated in the process of GC-decreased BMSC proliferation and osteoblastic differentiation.
Methods Western blot, quantitative real-time PCR, and cell proliferation and osteoblastic differentiation assays were employed to investigate the role of microRNAs in GC-inhibited BMSC proliferation and osteoblastic differentiation.
Results We found that microRNA-34a-5p was reciprocally regulated by Dex during the process of BMSC proliferation and osteoblastic differentiation. Furthermore, we confirmed that microRNA-34a-5p was a critical player in Dex-inhibited BMSC proliferation and osteogenic differentiation. Mechanistic studies showed that Dex inhibited BMSC proliferation by microRNA-34a-5p targeting cell cycle factors, including CDK4, CDK6, and Cyclin D1. Furthermore, down-regulation of microRNA-34a-5p by Dex leads to Notch signaling activation, resulting in inhibition of BMSC osteogenic differentiation.
Conclusions These results showed that microRNA-34a-5p, a crucial regulator for BMSC proliferation and osteogenic differentiation, might be used as a therapeutic target for GC-impaired bone formation.

Keywords Glucocorticoid · Marrow stromal stem cell · MicroRNA-34a-5p · Osteoblastic differentiation · Proliferation

H. Kang and H. Chen contributed equally to this work.

✉ L. Deng
lfdeng@msn.com

✉ L. Guo
guolei607@126.com

H. Kang
huik0216@163.com

H. Chen
wsyhch12@163.com

[1] Shanghai Key Laboratory for Bone and Joint Diseases, Shanghai Institute of Orthopaedics and Traumatology, Shanghai Ruijin Hospital, Shanghai Jiaotong University School of Medicine, Shanghai, China

[2] Ruijin Hospital, Shanghai Jiaotong University School of Medicine, No. 197, The Second Ruijin Road, Luwan District, Shanghai 200025, People's Republic of China

Introduction

Glucocorticoids (GCs) are used most extensively as anti-inflammatory and immunosuppressive drugs for treating a variety of diseases such as inflammation, cancer, and

autoimmune disorders [1, 2]. Although GCs are used extensively to relieve these diseases, prolonged use of GCs is associated with several serious side effects such as osteoporosis [3]. GC-induced osteoporosis (GCOP) is often the etiology of secondary osteoporosis (OP) [4]. Bone changes occur quickly after GC initiation, and it is estimated that up to half of patients treated with long-term GCs will fracture [5]. Although advances have been made over the past decade, cellular and molecular mechanisms involved in the determination of the levels of reduction in bone, due to GC excess, are not yet fully understood.

It is well known that bone remodeling is attributed to a dynamic metabolic balance between the destruction of preexisting bone by osteoclasts and rebuilding by osteoblasts [6]. It is generally accepted that inhibition of bone formation with impaired osteoblastic cell proliferation, differentiation, and function is the predominant effect of GCs on bone turnover [5]. Osteoblasts originate from stem cells within the bone marrow stroma lying on the abluminal surface of bone marrow sinusoids and are termed bone marrow stromal (skeletal or mesenchymal) stem cells (MSCs). MSCs can be recruited and located within the bone marrow near the bone formation surfaces to mediate osteogenesis [7]. GC-decreased bone formation is the result of inefficient proliferation or differentiation of MSCs into osteoblast cells [8]. Therefore, identifying factors regulating MSC proliferation and osteoblastic differentiation by GCs is an area of intensive investigation with potential for identifying novel targets to enhance bone formation for GCOP treatment.

Recently, noncoding microRNAs (miRNAs) have emerged as important gene expression regulatory elements. MiRNAs are single-stranded RNAs 19–25 nucleotides in length that regulate several pathways including the development timing, hematopoiesis, organogenesis, apoptosis, cell proliferation, and tumorigenesis [9, 10]. MiRNAs affect gene expression through the inhibitory engagement of complimentary "seed sequences" within the 3′-untranslational region (3′-UTR) of target messenger RNAs (mRNAs), resulting in translational inhibition and/or mRNA degradation. The miRNAs may also increase translation of selected mRNAs in a cell cycle-dependent manner [11]. Recently, studies have shown an important role of miRNAs in GC-mediated responses in various cellular processes, including cell proliferation, apoptosis, and differentiation [12–14]. Furthermore, some studies have covered the role of miRNAs in regulating osteogenesis, including miR-199a, miR-34a-5p, miR-27a, and miR-138 [13, 15–17]. However, the question of whether these molecules are implicated in the process of GC-repressed MSC proliferation and osteoblastic differentiation is still unanswered.

In this study, we examined the role of miR-34a-5p in the repression of MSC proliferation and osteoblastic differentiation by GCs. We profiled the genome-wide miRNA expression during GC-inhibited MSC proliferation. Several altered miRNAs were suggested, in which miR-34a-5p was identified as a strong candidate responsible for MSC proliferation. Furthermore, further studies found that miR-34a-5p was also involved in GC-decreased MSC osteoblastic differentiation. Therefore, miRNAs and miRNA-mediated gene silencing may contribute to inhibition effects of GCs on MSC proliferation and osteoblastic differentiation.

Materials and methods

In vivo treatment of mice

All procedures involving mice were approved by the Shanghai Jiaotong University Animal Study Committee and were carried out in accordance with the guide for the humane use and care of laboratory animals. According to Li et al.'s report [18], 8-week-old C57 male mice were injected intraperitoneally once daily with dexamethasone (Dex) sodium phosphate injection solution (50 mg/kg body weight) or with saline as a control for a period of 5 weeks. After the last injection, the mice were killed by cervical dislocation within 24 h. Bone marrow cells from the tibia and femur of mice injected with Dex were flushed out with Dulbecco's Modified Eagle's Medium (D-MEM) and cultured in growth medium (D-MEM containing 10 % FBS, 1 % penicillin-streptomycin (all from Hyclone, Logan, UT, USA)) at 37 °C in the presence of 5 % CO_2, following lysis of red blood cells. Nonadherent cells were removed by replacing the medium after 1 day.

Skeletal phenotyping

The distal end of intact femurs from control and Dex mice was scanned using micro-CT (GE Locus SP) to assess bone mass, density, and trabecular microarchitecture. Parameters computed from these data include bone mineral density (BMD) and trabecular number (Tb.N).

Immunohistochemistry

Femur sections were quenched with 3 % hydrogen peroxide for 15 min to reduce endogenous peroxide activity and blocked with 3 % normal goat serum in Tris-buffered saline. The sections were then incubated with rabbit anti-mouse Runx2, Osterix polyclonal antibodies (Santa Cruz Biotechnology, CA) at 4 °C overnight, followed by biotinylated secondary antibodies and a peroxidase-labeled streptavidin-biotin staining technique (DAB kit, Invitrogen). Nuclei were counterstained with hemalum (FARCO Chemical Supplies, Hong Kong). The slides were visualized by a microscope (ZEISS, AXIO). The slides without incubation with secondary antibody were used as negative controls.

Cell culture

Mouse MSCs (mMSCs), isolated from the bone marrow of C57BL/6 mice, were obtained from Cyagen Biosciences Inc (China). Identification of the cells according to the cell surface phenotypes and multipotency was performed by the supplier. mMSCs were cultured with alpha-Minimal Essential Media (α-MEM) (Invitrogen, Paisley, UK) supplemented with 10 % fetal bovine serum (FBS) and 100 μg/ml penicillin/streptomycin. Human MSCs (hMSCs) were obtained according to Chiu et al.'s reports [19]. Briefly, bone marrow aspirates were obtained aseptically from four donors (male, 45–65 years old) with informed consent. The aspirates were immediately mixed with sodium-heparin (10,000 U/ml) and diluted in five volumes of phosphate buffered saline. The cell suspension was centrifuged and plated onto a 10-cm dish containing 10 ml D-MEM with 10 % FBS and 1 % penicillin-streptomycin. Osteoblastic differentiation of MSC was carried out using osteoblastic induction medium (OIM) containing standard growth medium supplemented with 10^{-8} M Dex, 50 μg/ml ascorbic acid, and 10 mM β-glycerophosphate (Sigma-Aldrich, St. Louis, USA).

Cell viability assay

Cell counting kit (CCK-8) assay was used to measure cell proliferation and viability. mMSCs were resuspended in a 200-μl cell culture medium and seeded at a density of 1×10^3 cells/ml in 96-well microtiter plates, incubated overnight for cell attachment. Ten microliters of CCK-8 reagent (Dojindo Laboratories, Japan) was added to each well 1 h before the end of incubation. The optical density (OD) value of each sample was measured at a wavelength of 450 nm on a microplate reader. The result of cell viability measurement is expressed as the absorbance at OD450. Control cells were treated in the same way, and the value of absorbance was defined as 100 % survival.

5-Ethynil-2′-deoxyuridine assay

Logarithmic growth-phase cells were seeded in 24-well plates and incubated with serum-free α-MEM for 24 h. In brief, 5-ethynil-2′-deoxyuridine (EdU) (Sigma-Aldrich, St. Louis, USA) solution was added to cell culture medium to a final concentration of 1:1000 and then incubated for 2 h. A cell fixative (containing 4 % paraformaldehyde in PBS) was added before incubation at room temperature for 30 min. After washing cells with PBS for two times, click reaction buffer (Tris-HCl, pH 8.5, 100 mM; $CuSO_4$, 1 mM; Apollo 550 fluorescent azide, 100 μM; ascorbic acid, 100 mM) was added for 10–30 min while protecting from light. Then, cells were washed with 0.5 % Triton X-100 for three times and stained subsequently with Hoechst (5 μg/ml) for 30 min at room temperature. Samples were stored in the dark at 4 °C prior to fluorescence microscopy (Olympus). EdU-positive cells were calculated with (EdU add-in cells/Hoechst-stained cells)×100 %.

5-(and-6)-Carboxyfluorescein diacetate succinimidyl ester assay

mMSC proliferation was measured by 5-(and-6)-carboxyfluorescein diacetate succinimidyl ester (CFSE) staining and flow cytometry [13]. mMSCs were incubated with CFSE (Invitrogen, Paisley, UK) at a concentration of 5 μmol/l in PBS for 15 min at 37 °C. The reaction was stopped by adding fetal calf serum. Cells were replated at a density of 48,000/well in six-well dishes and incubated with a different treatment for 3 days. After preparation by trypsinization and washing, fluorescence intensity was measured on a flow cytometer using excitation at 488 nm at the FL1 detection channel and analyzed with CellQuest software.

Alkaline phosphatase and alizarin red S staining

mMSCs were seeded onto six-well plates at 1×10^5 cells per well. After the cells reached confluence, the medium was changed to induction medium containing 50 μg/ml ascorbic acid, 10 mM β-glycerophosphate, and 10^{-8} M Dex. The cells were cultured for 7 or 14 days and then subjected to alkaline phosphatase (ALP) or alizarin red S (ARS) staining. All procedures were performed according to the manufacturer's instructions. Briefly, the cells were washed three times with PBS, fixed with 4 % paraformaldehyde for 15 min, and stained with ALP reagent or 0.2 % ARS solution for 30 min at 37 °C. After washing three times with distilled water, the stained cells in each well were photographed. Stainings were repeated for at least three times independently.

ALP activity

mMSCs were cultured in a 24-well plate with differentiation medium for 7 days. For quantitative ALP measurements, mMSCs were lysed using 100 μl RIPA lysis buffer, and the cell supernatant was collected into a 96-well plate. The ALP activity in the supernatant was evaluated with the Alkaline Phosphatase Assay Kit (Beyotime Biotech Inc., Jiangsu, China). After co-incubation of substrates and *p*-nitrophenol for 30 min at 37 °C, the ALP activity was determined at the wavelength of 405 nm. Finally, the ALP levels were normalized to the total protein content determined by the bicinchoninic acid Protein Assay Kit (Beyotime Biotech Inc., Jiangsu, China).

MicroRNA microarray analysis

Quiescent (growth-arrested) mMSCs cultured in 0.3 % FBS-α-MEM were divided into two groups: control group and Dex group. Control group cells were cultured in normal culture medium. Dex group cells were treated with 10^{-6} M Dex for 3 days. Following treatment, total RNA was isolated from untreated samples and Dex-treated samples. Five micrograms of total RNA from each sample was labeled and hybridized on microRNA microarray chips as previously described [20].

Western blot analysis

The protein samples were extracted from cells. Protein samples (~50 μg) were fractionated by SDS-PAGE (7.5–10 % polyacrylamide gels). Separated proteins were blot transferred onto a nitrocellulose membrane. After blocking with 0.1 % Tween 20 and 5 % nonfat dry milk in Tris-buffered saline at room temperature for 1 h, the membrane was incubated overnight at 4 °C in one of the following primary antibodies: CDK4 (Peprotech, Rocky Hill, NJ) (1:400), CDK6 (Santa Cruz, CA, USA), Cyclin D1, JAG1, and β-actin (Santa Cruz, CA, USA) (1:500) as an internal control. The membrane was incubated with horseradish peroxidase-conjugated secondary antibody (1:5000) for 2 h and detected using the Enhanced Chemiluminescence Western blot System (Amersham Biosciences).

Synthesis and transfection of sequences of miR-34a-5p/AMO-34a-5p

MiR-34a-5p (sense: 5′-UGGCAGUGUCUUAGCUGGUUGU-3′, antisense: 5′-UCCCGUCAUAUGAACGAC UAA-3′) and its antisense oligonucleotides (AMOs: 5′-ACAACCAGCTAAGACACTGCCA-3′) were synthesized by Integrated DNA Technologies. Additionally, a scrambled RNA was used as negative control (NC), sense: 5′-UUCUCCGAACGUGUCACGUTT-3′ and antisense: 5′-ACGUGACACGUUCGGAG AATT-3′. The mMSCs were transfected with miR-34a-5p or/and inhibitors for 48 h under normal/differentiation condition, with X-tremeGENE small interfering RNA (siRNA) Transfection Reagent (Roche, Basel, Switzerland), according to the manufacturer's instructions.

Quantitative real-time PCR

Total RNA was extracted from mMSCs and hMSCs using the Trizol reagent (Invitrogen) according to the manufacturer's instructions. For reverse transcription of miR-34a-5p and mRNA, first-strand complementary DNA (cDNA) was synthesized from 1 μg of total RNA using PrimeScript RT reagent kits: Cat#RR037A and Cat#RR036A (TaKaRa, Dalian, China), respectively. After reverse transcription reaction, real-time PCR was performed using a SYBR Green qRT-PCR kit (TaKaRa, Dalian, China) and an ABI Step One Plus Real-Time PCR System. U6 and β-actin were respectively used as references for quantitation of miR-34a-5p and mRNAs. The primer sequences used in this study were as follows: U6: RT, 5′-CGCTTCACGAATTTGCGTGTCAT-3′; forward, 5′-CAAAGTGCTTACAGTGCAGGTAG-3′; reverse, 5′-CTACCTGCACTGTAAGCACTTTG-3′; miR-34a-5p: RT, 5′-GTCGTATCCAGTGCGTGTCGTGGAGTCGGCAATTGC-ACTGGATACGACACAACCA-3′; forward, 5′-GGGTGGCAGTGTCTTAGC-3′; reverse, 5′-CAGTGCGTGTCGTGGAGT-3′; Osterix (accession no. AF184902.1): forward, 5′-GTCCTCTCTGCTTGAGGAAGAA-3′; reverse, 5′-GGGCTGAAAGGTCAGC GTAT-3′; Runx2 (accession no. NM_009820.5): forward, 5′-GTGTCACTGCGCTGAAGAGG-3′; reverse, 5′-GACCAACCGAGTCATTTAAGGC-3′; ALP (accession no. X13409.1): forward, 5′-GGTAGATTACGCTCAC AACAA-3′; reverse, 5′-A GGCATACGCCATCACAT-3′; OC (accession no. X04142.1): forward, 5′-ACCCT GGCTGCGCTCTGTCTCT-3′; reverse, 5′-AGGTAGCGCCGGAGTCTGTTCAC-3′; and β-actin (accession no. NM_007393.4): forward, 5′-CTGTCCCTGTATGCCTCTG-3′; reverse, 5′-ATGTCACGCACGATTTCC-3′.

Statistics

The composite data are expressed as means±sem. Statistical analysis was performed with one-way ANOVA followed by Dunnett's test where appropriate. Differences were considered to be significant at $P \leq 0.05$.

Results

The effect of Dex on mMSC proliferation and osteoblastic differentiation

To determine whether Dex regulated mMSC proliferation, we firstly used CCK-8 assay to monitor cell viability. mMSCs were cultured in normal medium with Dex at different concentrations (0, 10^{-8}, 10^{-7}, and 10^{-6} M) from day 1 to day 3. Our results showed that Dex decreased the viability of mMSCs in a dose- and time-dependent manner (Fig. 1a).

Furthermore, mMSCs were stimulated with 10^{-6} M Dex for 3 days prior to EdU assay. EdU-stained photomicrographs and corresponding photomicrographs of total cells are shown in Fig. 1b. The proportion of cells with EdU-positive nuclei is shown in Fig. 1c. EdU incorporation was decreased in the Dex group, indicating that Dex could inhibit the mMSC proliferation.

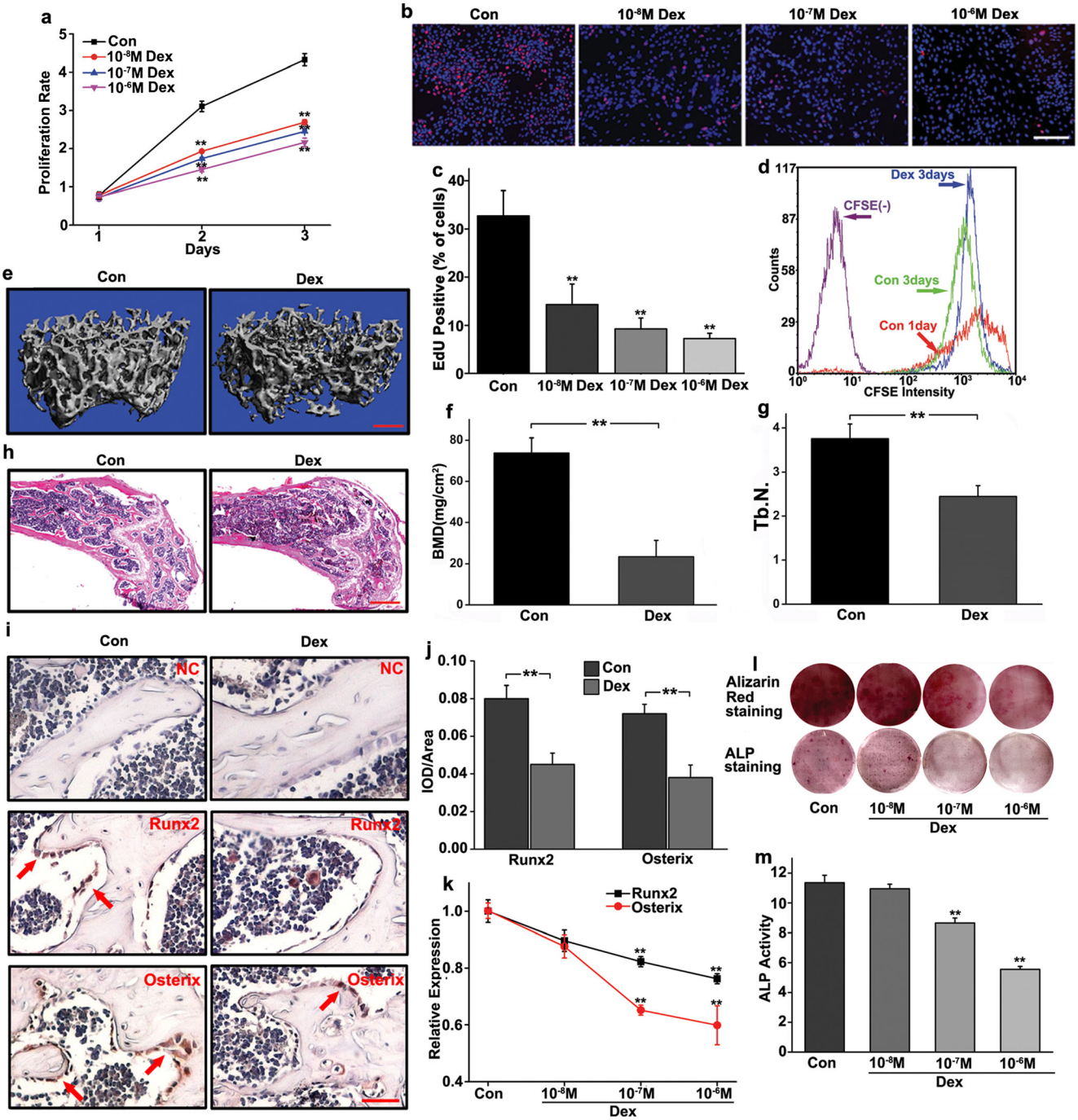

Fig. 1 The inhibition of mMSC proliferation and osteoblastic differentiation by Dex. **a** Proliferation of mMSCs was measured by CCK-8 after cells were treated with 10^{-8}, 10^{-7}, and 10^{-6} M Dex from day 1 to day 3. n=3, $^{**}P$<0.01. **b** Representative photomicrographs of EdU staining. *Blue* marks the Hoechst labeling of cell nuclei and *red* marks EdU labeling of nuclei of proliferative cells (×200). *Scale bars* are 50 μm. **c** Quantitative data showing the percentage of EdU-positive cells in different treatment groups (number of *red* vs number of *blue* nuclei). n=3, $^{**}P$<0.01. **d** mMSCs were stained with CFSE before plating, cultured for 3 days, and analyzed by flow cytometry as described in "Materials and methods." n=3. **e** Representative figures of micro-CT analysis of the distal end of intact femurs of mice treated with Dex. *Scale bars* are 25 μm. **f** BMD in the distal end of intact femurs of each experimental group. n=4, $^{**}P$<0.01. **g** Tb.N in the distal end of intact femurs of each experimental group. n=4, $^{**}P$<0.01. **h** Hematoxylin-eosin staining was performed to histologically identify structures of the distal end of intact femurs of mice injected with Dex for 5 weeks. *Scale bars* are 50 μm. **i**, **j** Runx2 and Osterix expression and localization (*red arrow*) in the distal end of intact femurs of each experimental group through immunohistochemistry. *Scale bars* are 20 μm. n=4, $^{**}P$<0.01. **k** qRT-PCR analysis of *Runx2* and *Osterix* expression in mMSCs induced by osteoblastic differentiation medium and treated with Dex for 3 days. n=4, $^{**}P$<0.01. **l** Dex inhibited osteogenic differentiation of mMSCs in a dose-dependent manner, as evidenced by changes in mineralized matrix formation (ARS staining, day 14) and ALP staining (day 7). **m** Dex inhibited osteogenic differentiation of mMSCs in a dose-dependent manner, as evidenced by changes in ALP activity (day 7)

To further examine proliferation, mMSCs were cultured with 10^{-6} M Dex for 3 days and stained with CFSE. CFSE irreversibly couples to cellular proteins. When cells divide, CFSE labeling is distributed equally between daughter cells, which are half as fluorescent as their parents. The peak CFSE fluorescence intensity on flow cytometry was right shifted by Dex, indicating that mMSCs treated with Dex had fewer cycles of cell replication as compared with the control group (Fig. 1d).

Next, we investigated the effect of Dex on mMSC osteoblastic differentiation. Eight-week-old mice were injected with Dex for 5 weeks to generate a Dex mice model. Micro-CT analysis of distal femur metaphysis revealed that the BMD and Tb.N of Dex mice were significantly lower compared to those of control mice (Fig. 1e–g), in consistence with the less amount of trabecular bones shown in HE staining (Fig. 1h). The master osteogenic transcription factors Runx2 and Osterix were significantly decreased in osteoblasts on the surfaces of the trabecular bone in Dex mice (Fig. 1i, j). Subsequently, mMSCs were cultured in osteogenic medium with Dex at the concentrations (0, 10^{-8}, 10^{-7}, and 10^{-6} M) for 3 days. We found that Dex remarkably decreased the expression of *Runx2* and *Osterix* in a dose-dependent manner (Fig. 1k). In addition, Dex inhibited mMSC osteogenic potential, as evidenced by ARS and ALP staining (Fig. 1l). Similarly, ALP activity was also decreased by Dex in a dose-dependent manner, when mMSCs were induced by osteogenic medium (Fig. 1m). Taken together, these results strongly suggest that Dex significantly decreases mMSC proliferation and osteoblastic differentiation.

Reciprocal regulation of miR-34a-5p expression by Dex in MSC proliferation and osteoblastic differentiation

To detect miRNAs related to Dex-decreased mMSC proliferation, microRNA expression was analyzed with a RNA/cDNA-based microarray screening. We analyzed a panel of mRNAs obtained from mMSCs subjected to a 10^{-6}-M Dex assault for 3 days. Among the miRNAs represented on our chip, nine were differentially expressed in response to Dex-decreased mMSC proliferation (Fig. 2a). To confirm the results of microarray-based screening, we measured the expressions of these identified miRNAs using quantitative real-time PCR (qRT-PCR). During these differentially expressed miRNAs, miR-34a-5p was found to be upregulated by more than fivefold (Fig. 2b). Further studies confirmed the upregulation of miR-34a-5p expression by Dex in a dose-dependent manner (Fig. 2c). Furthermore, the effects of Dex on miR-34a-5p expression were observed in hMSCs. In consistence with the results from mMSCs, Dex also greatly increased miR-34a-5p expression in hMSCs (Fig. 2d).

Next, we investigated the effects of Dex on miR-34a-5p expression during mMSC osteoblastic differentiation. Surprisingly, when mMSCs cultured under osteogenic medium were treated with 10^{-6} M Dex for 3 days, miR-34a-5p expression was significantly decreased (Fig. 2e). Similar results were also observed in hMSCs, when cells were cultured in osteogenic medium with 10^{-6} M Dex (Fig. 2f), indicating that Dex reciprocally regulated miR-34a-5p expression in MSC proliferation and osteoblastic differentiation. Furthermore, a significant inhibition of miR-34a-5p expression was also observed in MSCs from Dex mice (Fig. 2g).

The effect of miR-34a-5p on Dex-decreased mMSC proliferation

To delineate the role of miR-34a-5p in Dex-decreased mMSC proliferation, we performed loss-of-function and gain-of-function experiments in which we decreased and increased the quantities of miR-34a-5p with a miR-34a-5p inhibitor and a miR-34a-5p mimic, respectively. Then, we firstly assessed cell proliferation with CCK-8 assays. Our results showed that miR-34a-5p markedly facilitated Dex-decreased mMSC proliferation. Furthermore, the inhibitory effect of Dex on mMSC proliferation was significantly alleviated when mMSCs were transfected with AMO-34a-5p, indicating that miR-34a-5p was involved in Dex-decreased mMSC proliferation (Fig. 3a).

Furthermore, EdU assay by fluorescence microscopy further demonstrated that the miR-34a-5p mimic enhanced the inhibitory effects of Dex on mMSC proliferation, while the miR-34a-5p inhibitor alleviated it (Fig. 3b, c). Similar results were further confirmed by CFSE fluorescence intensity assay (Fig. 3d). Taken together, these results indicated that miR-34a-5p could be implicated in the process of Dex-decreased mMSC proliferation.

The effect of miR-34a-5p on Dex-decreased mMSC osteoblastic differentiation

To investigate whether miR-34a-5p was involved in Dex-decreased mMSC osteogenic differentiation, we observed the effect of Dex on osteoblastic differentiation of mMSCs transfected with miR-34a-5p or/and AMO-34a-5p. qRT-PCR results showed that the miR-34a-5p mimic clearly attenuated the inhibitory effect of Dex on the expressions of *Runx2*, *Osterix*, and *osteocalcin* (*OC*), while AMO-34a-5p greatly facilitated Dex-decreased expressions of *Runx2*, *Osterix*, and *OC* (Fig. 4a–c). In addition, ARS staining and ALP staining showed that overexpression of miR-34a-5p significantly attenuated the inhibitory effect of Dex on mMSC osteoblastic differentiation. However, miR-34a-5p depletion significantly facilitated Dex-decreased mMSC osteoblastic differentiation (Fig. 4d). Similar results were further confirmed by ALP activity assay (Fig. 4e), suggesting that miR-34a-5p was involved in Dex-decreased mMSC osteoblastic differentiation.

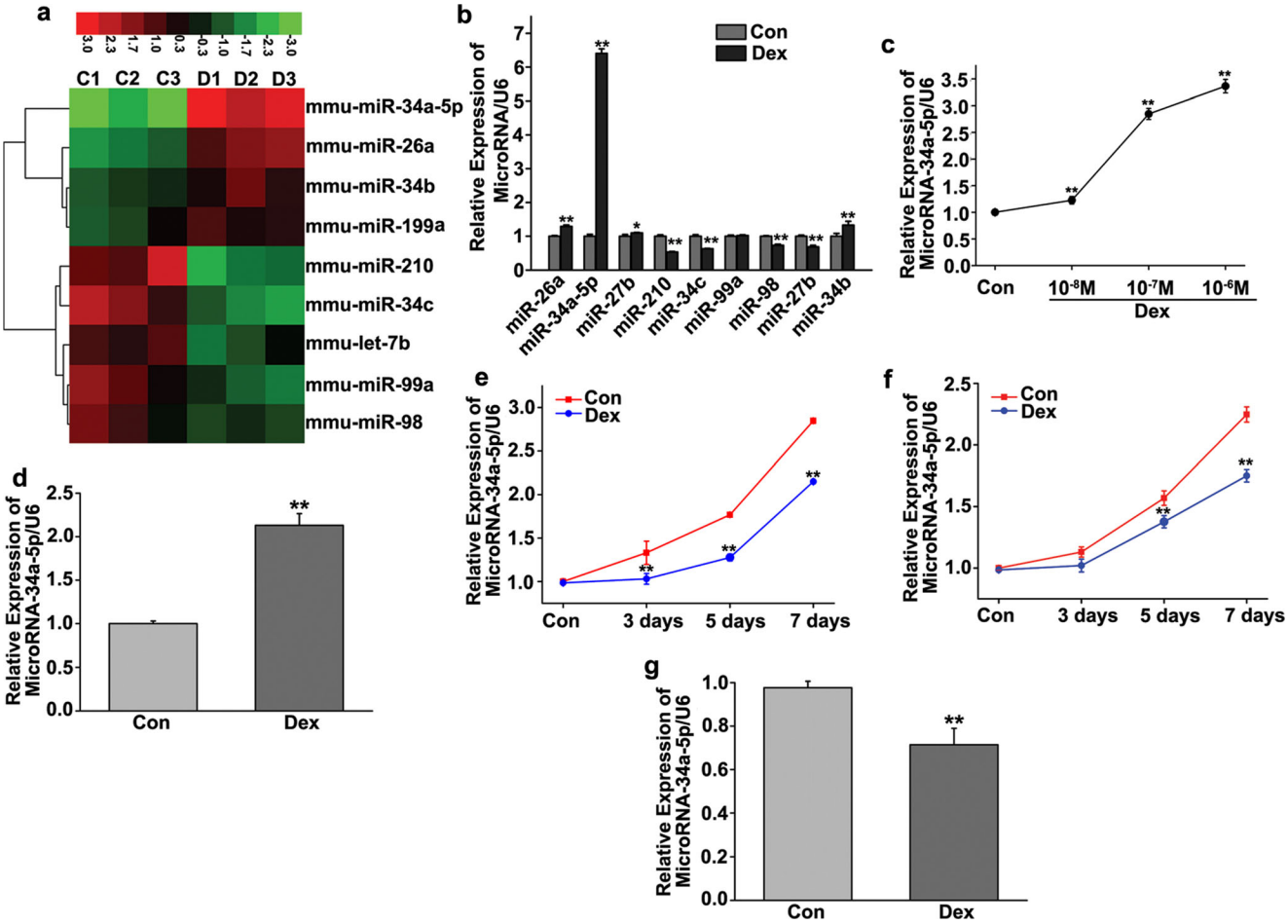

Fig. 2 Dex reciprocally regulated miR-34a-5p expression during MSC proliferation and osteogenic differentiation process. **a** Heat map representation of miRNAs differentially expressed in mMSCs treated with 10^{-6} M Dex for 3 days. *Red* indicates miRNAs induced, and *green* indicates miRNAs repressed. $n=3$. **b** Gene chip results were validated with qRT-PCR in mMSCs treated with 10^{-6} M Dex for 3 days. $n=3$, $^{**}P<0.01$, $^{*}P<0.05$. **c** Expression of miR-34a-5p was measured by qRT-PCR in mMSCs treated with 10^{-8}, 10^{-7}, and 10^{-6} M Dex. $n=3$, $^{**}P<0.01$, $^{*}P<0.05$. **d** Expression of miR-34a-5p was measured by qRT-PCR in hMSCs treated with 10^{-6} M Dex for 3 days. $n=3$, $^{**}P<0.01$. **e** Expression of miR-34a-5p was measured by qRT-PCR in mMSCs induced by osteogenic medium and treated with 10^{-6} M Dex from day 3 to day 7. $n=3$, $^{**}P<0.01$. **f** Expression of miR-34a-5p was measured by qRT-PCR in hMSCs induced by osteogenic medium and treated with 10^{-6} M Dex from day 3 to day 7. $n=3$, $^{**}P<0.01$. **g** Expression of miR-34a-5p was measured by qRT-PCR in mMSCs from Dex mice. $n=4$, $^{**}P<0.01$

Molecular targets of miR-34a-5p involved in Dex-decreased mMSC proliferation and osteoblastic differentiation

Based on the above observations, miR-34a-5p was involved in Dex-decreased mMSC proliferation and osteoblastic differentiation. It is possible that miR-34a-5p targets several regulatory factors associated with mMSC proliferation and osteoblastic differentiation. To address this issue, we used a computation and bioinformatics-based approach to predict the putative targets related to proliferation and osteoblastic differentiation through TargetScan, which is hosted by the Wellcome Trust Sanger Institute. These explorations lead to the identification of candidate targets of miR-34a-5p: cyclin-dependent kinase 4 (CDK4), CDK6, Cyclin D1, and jagged 1 (JAG1). Western blot analysis showed that the expressions of cell cycle factors, including CDK4, CDK6, and Cyclin D1, were greatly decreased in the mMSCs treated with 10^{-6} M Dex for 3 days. Overexpression of miR-34a-5p significantly increased the inhibitory effect of Dex on the expressions of CDK4, CDK6, and Cyclin D1, while AMO-34a-5p greatly alleviated the Dex-decreased expressions of cell cycle factors (Fig. 5a–c). These results suggested that Dex might decrease mMSC proliferation by miR-34a-5p targeting CDK4, CDK6, and Cyclin D1.

JAG1, a Notch ligand, was predicted as a potential target of miR-34a-5p involved in Dex-decreased mMSC osteoblastic differentiation. Our results showed that Dex significantly increased JAG1 expression. Furthermore, miR-34a-5p could alleviate the stimulatory effect of Dex on JAG1 expression. Conversely, inhibition of miR-34a-5p by AMO-34a-5p leads to greatly enhanced Dex-increased expression of JAG1

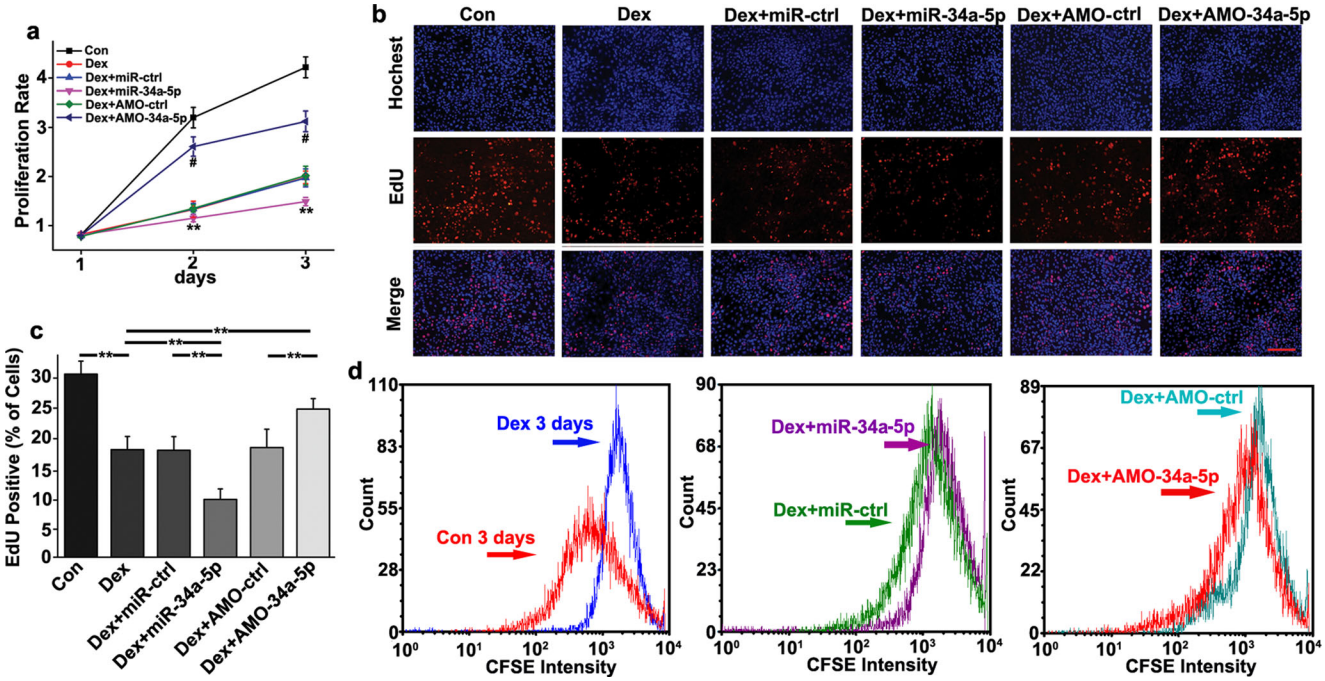

Fig. 3 Involvement of miR-34a-5p in Dex-decreased mMSCs proliferation. **a** Proliferation of mMSCs was measured by CCK-8 after cells were transfected with miR-34a-5p or/and AMO-34a-5p under 10^{-6} M Dex from day 1 to day 3. $n=3$, $^{**}P<0.01$ versus *Dex+miR-ctrl*; $\#P<0.01$ versus *Dex+AMO-ctrl*. **b** Representative photomicrographs of corresponding total cell photomicrographs (*top panel*) and EdU staining (*middle panel*). *Blue* marks DAPI labeling of cell nuclei and *red* marks EdU labeling of nuclei of proliferative cells (×200). *Scale bars* are 50 μm. **c** Quantitative data showing the percentage of EdU-positive cells in different treatment groups (number of *red* vs number of *blue* nuclei). $n=3$, $^{**}P<0.01$. **d** mMSCs were transfected with miR-34a-5p or/and AMO-34a-5p under 10^{-6} M Dex for 3 days, then cells were stained with CFSE and analyzed by flow cytometry as described in "Materials and methods." The *right shift of peak* of CFSE fluorescence intensity on flow cytometry indicated inhibition of cell replication. $n=3$

(Fig. 5d). Since JAG1 is a Notch-1 receptor ligand, we further identified whether Notch signaling was required for Dex-decreased mMSC osteogenic differentiation. Our results showed that Dex significantly inhibited the expressions of *Runx2*, *Osterix*, and *OC*, while blocking Notch signaling by JAG1-siRNA could alleviate the inhibitory effect of Dex on osteoblast marker gene expression (Fig. 6a–c), in consistence with the results shown in alizarin red staining, ALP staining, and activity assay (Fig. 6d, e). Taken together, these results indicated that Notch signaling activation was required for Dex-inhibited mMSC osteogenic differentiation.

Discussion

The inhibitory effects of GCs on MSC proliferation and osteoblastic differentiation are an important pathway through which GCs decrease bone formation. However, the cellular and molecular mechanism remains elusive. In this study, we identified that miR-34a-5p, a post-transcriptional regulator, was reciprocally regulated by Dex during the process of MSC proliferation and osteoblastic differentiation. We demonstrated that Dex might decrease MSC proliferation by miR-34a-5p targeting cell cycle factors, including CDK4, CDK6, and Cyclin D1. Furthermore, downregulation of miR-34a-5p by Dex leads to activation of Notch signaling, which decreased MSC osteoblastic differentiation.

Several recent reports have suggested that miRNAs and miRNA-mediated gene silencing contribute to GC-induced bone loss [13, 21]. Ko et al. reported that excess GC-induced loss of miR-29a signaling accelerated β-catenin deacetylation and ubiquitination that impairs osteogenic activities of osteoblast cultures [22]. Furthermore, miR-29a signaling protected against GC-induced disturbance of Wnt and Dkk-1 actions and improved osteoblast differentiation and mineral acquisition [23]. In addition, our previous studies showed that downregulation of miR-17~92a by GCs leads to Bim targeting and induction of osteoblast apoptosis [12]. Moreover, GCs could also increase receptor activator of nuclear factor B ligand (RANKL) expression through the downregulation of miR-17/20a in osteoblasts, which indirectly enhanced osteoclastogenesis and bone resorption [14]. However, to our knowledge, there have been no reports on whether miRNA expression could be regulated by GCs in MSC proliferation and osteoblastic differentiation. The present study is the first effort to observe the effect of GCs on miRNAs in MSC proliferation and osteoblastic differentiation.

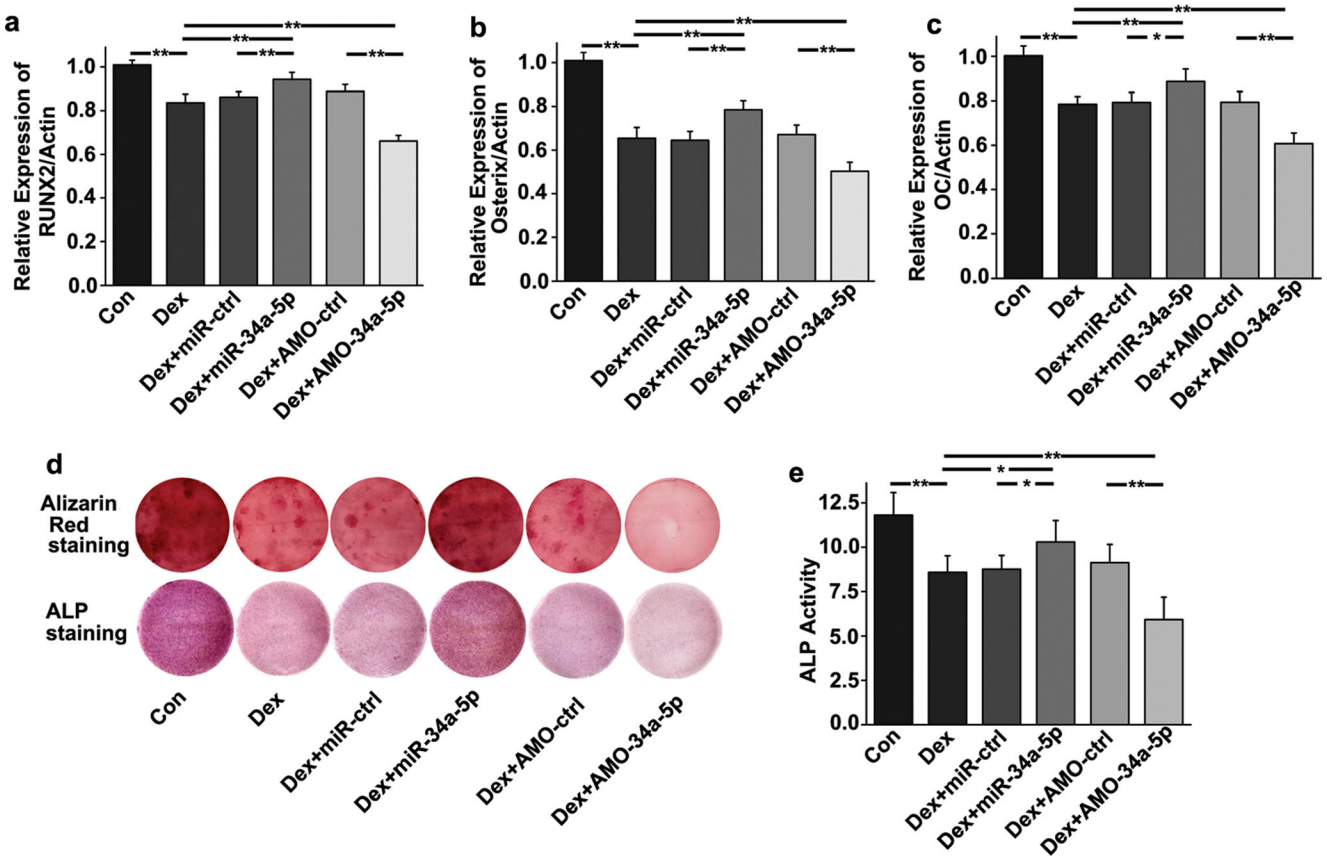

Fig. 4 Involvement of miR-34a-5p in Dex-decreased osteogenic differentiation of mMSCs. **a**, **b** qRT-PCR analysis of *Runx2* and *Osterix* expression in mMSCs transfected with miR-34a-5p or/and AMO-34a-5p under 10^{-6} M Dex and osteoblastic differentiation condition for 3 days. $n=3$, $^{**}P<0.01$. **c** qRT-PCR analysis of *OC* expression in mMSCs transfected with miR-34a-5p or/and AMO-34a-5p under 10^{-6} M Dex and osteoblastic differentiation condition for 7 days. $n=3$, $^{**}P<0.01$, $^{*}P<0.05$. **d** Osteogenic differentiation of mMSCs transfected with miR-34a-5p or/and AMO-34a-5p under 10^{-6} M Dex and osteoblastic differentiation conditions were observed by ARS staining (day 14) and ALP staining (day 7). $n=3$. **e** Osteogenic differentiation of mMSCs transfected with miR-34a-5p or/and AMO-34a-5p under 10^{-6} M Dex and osteoblastic differentiation conditions were measured by ALP activity (day 7). $n=3$, $^{**}P<0.01$, $^{*}P<0.05$

In this study, we found that miR-34a-5p was involved in the regulation of MSC proliferation and osteoblastic differentiation by GCs. Some results of our research were coincident with Chen et al.'s report that miRNA-34a exhibited unique dual regulatory effects controlling both hMSC proliferation and osteoblastic differentiation [15]. However, our results showed that miR-34a-5p as a positive regulator was implicated in Dex-decreased osteogenic differentiation of MSCs, which was just the opposite of Chen et al.'s report that miR-34a was a negative regulator for MSC osteoblastic differentiation. We presumed that miR-34a-5p might play different roles in MSCs exposed to different conditions. In addition, Chen et al. reported that miR-34a-5p affected MSC proliferation during the osteogenic differentiation process. However, our study revealed that miR-34a-5p was implicated in Dex-decreased MSC proliferation, when cells were cultured in normal medium, but not in osteogenic medium.

Previous studies showed that miR-34b and miR-34c affected skeletogenesis during embryonic development and inhibited osteoblast proliferation and terminal differentiation of osteoblasts [24]. Differential expressions of miR-34b and miR-34c were also observed in our study, although to a lesser extent. As the most robust change was miR-34a-5p, thus we firstly explored the roles of miR-34a-5p on Dex-regulated MSC proliferation and osteoblastic differentiation. It is also possible that even though a member of the miR-34a-5p family might be involved in osteoblast proliferation and differentiation, only miR-34a-5p might dominantly contribute to the inhibitory effects of GCs on MSC proliferation and osteoblastic differentiation. Future studies will be required to explore the effects of miR-34b and miR-34c on Dex-regulated proliferation and osteogenic differentiation of MSCs.

GCs, which regulate diverse physiological effects, have established both genomic and nongenomic mechanisms. Although GCs appear to mediate some rapid, nongenomic cellular responses by interacting with membrane receptors, classical, intracellular GR that functions as ligand-activated transcription factors mediates many GC responses [25]. Wei

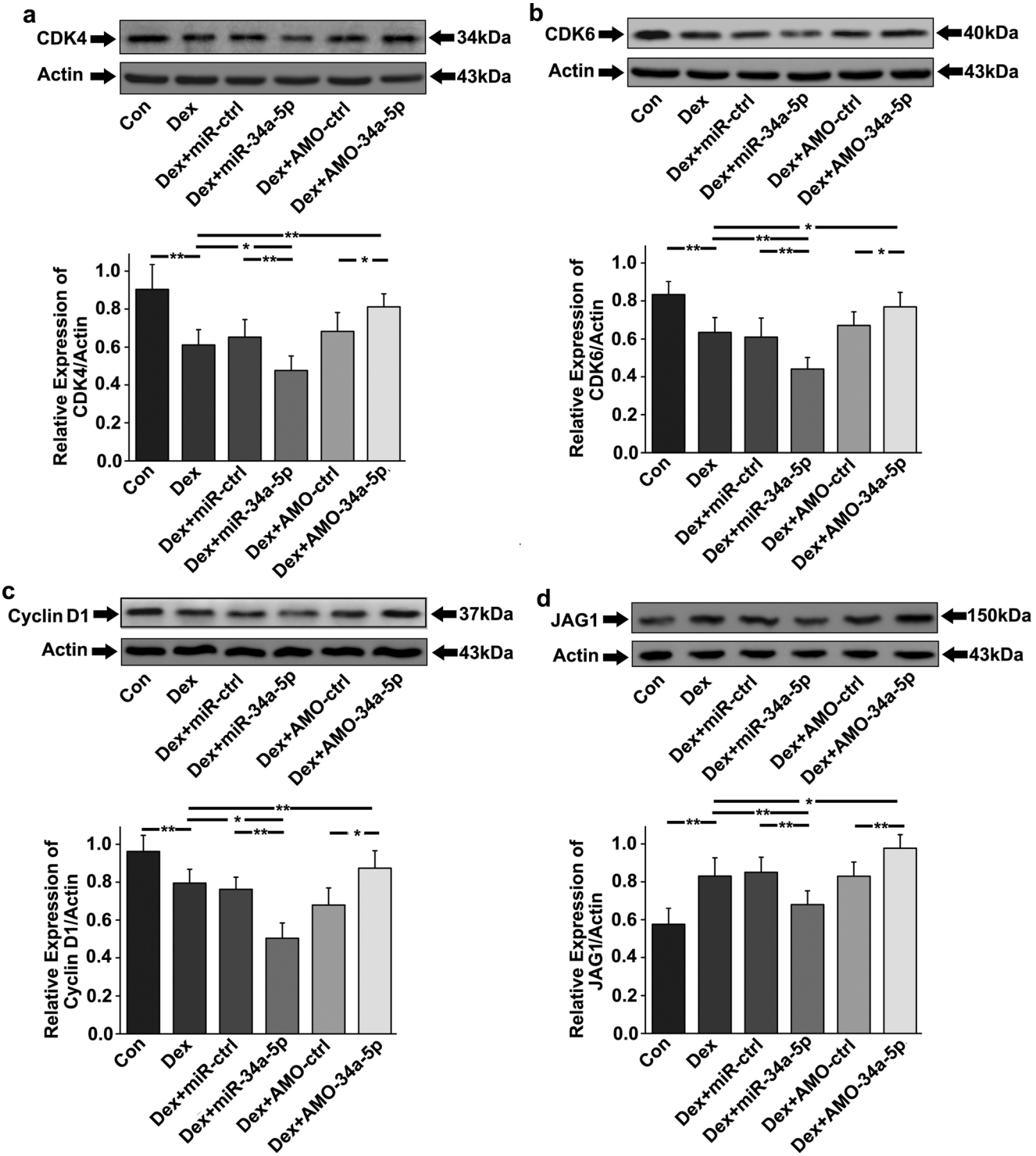

Fig. 5 Identification of target genes regulated by miR-34a-5p in Dex-decreased mMSC proliferation and osteogenic differentiation. **a** Western blot analysis of CDK4 expression in mMSCs transfected with miR-34a-5p or/and AMO-34a-5p under 10^{-6} M Dex for 3 days. n=3, $^{**}P<0.01$, $^{*}P<0.05$. **b** Western blot analysis of CDK6 expression in mMSCs transfected with miR-34a-5p or/and AMO-34a-5p under 10^{-6} M Dex for 3 days. n=3, $^{**}P<0.01$, $^{*}P<0.05$. **c** Western blot analysis of Cyclin D1 expression in mMSCs transfected with miR-34a-5p or/and AMO-34a-5p under 10^{-6} M Dex for 3 days. n=3, $^{**}P<0.01$, $^{*}P<0.05$. **d** Western blot analysis of JAG1 expression in mMSCs transfected with miR-34a-5p or/and AMO-34a-5p under 10^{-6} M Dex and osteoblastic differentiation condition for 7 days. n=3, $^{**}P<0.01$, $^{*}P<0.05$

et al. reported that the inhibitory effects of GCs on MSC proliferation and differentiation were remarkably attenuated by blocking GR expression [26]. Therefore, GC-inhibited proliferation and differentiation of MSCs are triggered via GR-

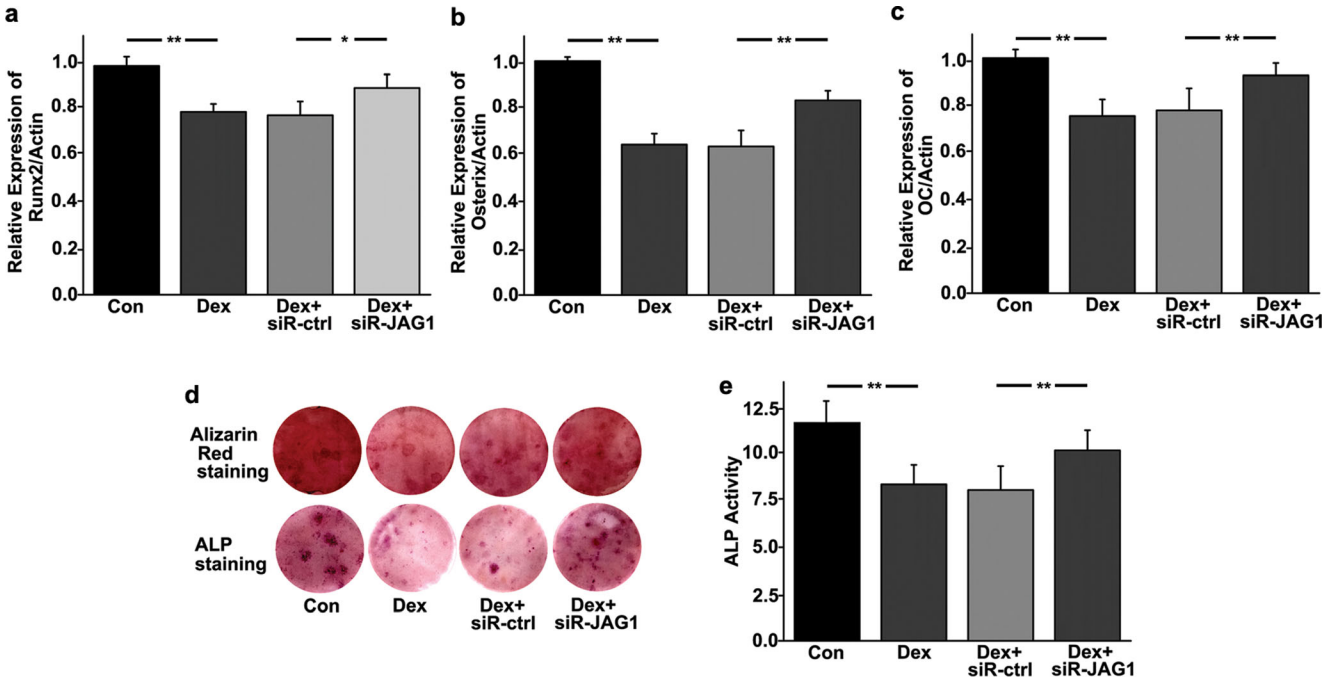

Fig. 6 Notch signaling pathway activation was required for Dex-decreased osteogenic differentiation of mMSCs. **a**, **b** qRT-PCR analysis of *Runx2* and *Osterix* expression in mMSCs transfected with siR-ctrl/siR-JAG1 under 10^{-6} M Dex and osteoblastic differentiation condition for 3 days. $n=3$, $^{**}P<0.01$, $^{*}P<0.05$. **c** qRT-PCR analysis of *OC* expression in mMSCs transfected with siR-ctrl/siR-JAG1 under 10^{-6} M Dex and osteoblastic differentiation condition for 7 days. $n=3$, $^{**}P<0.01$, $^{*}P<0.05$. **d** Osteoblast differentiation of mMSCs transfected with siR-ctrl/siR-JAG1 under 10^{-6} M Dex and osteoblastic differentiation conditions were observed by ARS staining (day 14) and ALP staining (day 7). $n=3$. **e** Osteoblast differentiation of mMSCs transfected with siR-ctrl/siR-JAG1 under 10^{-6} M Dex and osteoblastic differentiation conditions were measured by ALP activity (day 7). $n=3$, $^{**}P<0.01$, $^{*}P<0.05$

dependent transcriptional regulation. Previous study reported that GCs could regulate miRNA expression via a GR-mediated direct DNA binding mechanism [27]. In this study, we did not uncover the mechanisms of GC-mediated miR-34a-5p expression in MSCs. Therefore, future studies need to be done to explore the progress of GC-regulated miR-34a-5p expression.

Previous studies showed that a number of cell cycle genes and proliferation proteins, such as Cyclin D1, CDK4, CDK6, E2F transcription factor three (E2F3), and cell division cycle 25 homolog A (Cdc25A), were among the miR-34a-5p targets, which were crucial players for MSC proliferation [15]. However, our results confirmed that Dex could inhibit mMSC proliferation by miR-34a-5p targeting Cyclin D1, CDK4, and CDK6, but not E2F3 and Cdc25A (data were not shown). These results suggested that the role of miR-34a-5p target genes in mMSC proliferation was different, when cells were exposed to different conditions.

JAG1 as a target gene of miR-34a-5p was implicated in the Dex-inhibited differentiation of MSCs into osteoblasts. JAG1 interacting with Notch receptors leads to release of the Notch intracellular domain (NICD), allowing it to translocate into the nucleus and activate Notch-responsive genes that are important for cell differentiation and morphogenesis in different biological systems [28]. Indeed, the role of Notch signaling in MSC osteoblastic differentiation and bone formation has yielded conflicting results [29–32]. We found that activation of the Notch signaling pathway was involved in Dex-inhibited mMSC osteoblastic differentiation. Furthermore, Xu et al. found that activation of Notch signaling was involved in hypoxia-inhibited mMSC osteoblastic differentiation [33]. However, Chen et al. showed that activation of the Notch signaling pathway could promote osteogenic differentiation of hMSCs [15]. Taken together, it is possible that activation of the Notch signaling pathway under different conditions might carry out opposite roles in MSC osteoblastic differentiation. Furthermore, Zhu et al. suggested that JAG1 was sufficient to induce osteoblast differentiation in hMSCs, while conversely inhibiting osteoblastogenesis in mMSCs [34]. Therefore, it is also likely that the roles of the Notch signaling pathway in MSC osteogenic differentiation might be different, when MSCs were derived from different species.

Our data provide new evidence that miR-34a-5p as a dual-effector miRNA was involved in the inhibitory effects of GCs on MSC proliferation and osteoblastic differentiation. Upregulation of miR-34a-5p by GCs leads

to cell cycle gene (Cyclin D and CDK4) targeting and inhibition of MSC proliferation. Furthermore, downregulation of miR-34a-5p by GCs caused activation of the Notch signaling pathway and inhibition of MSC osteoblastic differentiation. Thus, this study is an effort to establish a molecular mechanism of GC-induced bone loss and to provide insights into the potential contribution of miRNA in the regulation of MSC proliferation and osteoblastic differentiation by GCs.

Acknowledgments This work was supported by the National Natural Science Foundation of China (grant numbers: 81300713, 81371958); Innovation Program of Shanghai Municipal Education Commission (grant number: 14YZ044); Basic Key Project of Shanghai (grant number: 12JC140820); and Shanghai Municipal Science and Technology Commission Biomedicine Technology Support Project (grant number: 13431900702).

Compliance with ethical standards All procedures involving mice were approved by the Shanghai Jiaotong University Animal Study Committee and were carried out in accordance with the guide for the humane use and care of laboratory animals.

Conflicts of interest None.

References

1. Shi C, Qi J, Huang P et al (2014) MicroRNA-17/20a inhibits glucocorticoid-induced osteoclast differentiation and function through targeting RANKL expression in osteoblast cells. Bone 67–75
2. Tait AS, Butts CL, Sternberg EM (2008) The role of glucocorticoids and progestins in inflammatory, autoimmune, and infectious disease. J Leukoc Biol 84:924–931
3. Kondo T, Kitazawa R, Yamaguchi A, Kitazawa S (2008) Dexamethasone promotes osteoclastogenesis by inhibiting osteoprotegerin through multiple levels. J Cell Biochem 103:335–345
4. Weinstein RS, Jilka RL, Parfitt AM, Manolagas SC (1998) Inhibition of osteoblastogenesis and promotion of apoptosis of osteoblasts and osteocytes by glucocorticoids. Potential mechanisms of their deleterious effects on bone. J Clin Invest 102:274–282
5. Henneicke H, Gasparini SJ, Brennan-Speranza TC, Zhou H, Seibel MJ (2014) Glucocorticoids and bone: local effects and systemic implications. Trends Endocrinol Metab TEM 25:197–211
6. Lemaire V, Tobin FL, Greller LD, Cho CR, Suva LJ (2004) Modeling the interactions between osteoblast and osteoclast activities in bone remodeling. J Theor Biol 229:293–309
7. Sacchetti B, Funari A, Michienzi S et al (2007) Self-renewing osteoprogenitors in bone marrow sinusoids can organize a hematopoietic microenvironment. Cell 131:324–336
8. Mitra R (2011) Adverse effects of corticosteroids on bone metabolism: a review. PM R 3:466–471, **quiz 471**
9. Couzin J (2007) Genetics. Erasing microRNAs reveals their powerful punch. Science 316:530
10. Zamore PD, Haley B (2005) Ribo-gnome: the big world of small RNAs. Science 309:1519–1524
11. Zeng Y (2006) Principles of micro-RNA production and maturation. Oncogene 25:6156–6162
12. Guo L, Xu J, Qi J, Zhang L, Wang J, Liang J, Qian N, Zhou H, Wei L, Deng L (2013) MicroRNA-17-92a upregulation by estrogen leads to Bim targeting and inhibition of osteoblast apoptosis. J Cell Sci 126:978–988
13. Shi C, Huang P, Kang H, Hu B, Qi J, Jiang M, Zhou H, Guo L, Deng L (2015) Glucocorticoid inhibits cell proliferation in differentiating osteoblasts by microRNA-199a targeting of WNT signaling. J Mol Endocrinol 54:325–337
14. Shi C, Qi J, Huang P et al (2014) MicroRNA-17/20a inhibits glucocorticoid-induced osteoclast differentiation and function through targeting RANKL expression in osteoblast cells. Bone 68:67–75
15. Chen L, Holmstrom K, Qiu W, Ditzel N, Shi K, Hokland L, Kassem M (2014) MicroRNA-34a inhibits osteoblast differentiation and in vivo bone formation of human stromal stem cells. Stem Cells 32:902–912
16. Pan W, Wang H, Jianwei R, Ye Z (2014) MicroRNA-27a promotes proliferation, migration and invasion by targeting MAP2K4 in human osteosarcoma cells. Cell Physiol Biochem 33:402–412
17. Eskildsen T, Taipaleenmaki H, Stenvang J, Abdallah BM, Ditzel N, Nossent AY, Bak M, Kauppinen S, Kassem M (2011) MicroRNA-138 regulates osteogenic differentiation of human stromal (mesenchymal) stem cells in vivo. Proc Natl Acad Sci U S A 108:6139–6144
18. Li J, Zhang N, Huang X, Xu J, Fernandes JC, Dai K, Zhang X (2013) Dexamethasone shifts bone marrow stromal cells from osteoblasts to adipocytes by C/EBPalpha promoter methylation. Cell Death Dis 4, e832
19. Chiu LH, Lai WF, Chang SF, Wong CC, Fan CY, Fang CL, Tsai YH (2014) The effect of type II collagen on MSC osteogenic differentiation and bone defect repair. Biomaterials 35:2680–2691
20. Dore LC, Amigo JD, Dos Santos CO et al (2008) A GATA-1-regulated microRNA locus essential for erythropoiesis. Proc Natl Acad Sci U S A 105:3333–3338
21. Kong X, Yu J, Bi J et al (2015) Glucocorticoids transcriptionally regulate miR-27b expression promoting body fat accumulation via suppressing the browning of white adipose tissue. Diabetes 64:393–404
22. Ko JY, Chuang PC, Chen MW, Ke HC, Wu SL, Chang YH, Chen YS, Wang FS (2013) MicroRNA-29a ameliorates glucocorticoid-induced suppression of osteoblast differentiation by regulating beta-catenin acetylation. Bone 57:468–475
23. Wang FS, Chuang PC, Lin CL, Chen MW, Ke HJ, Chang YH, Chen YS, Wu SL, Ko JY (2013) MicroRNA-29a protects against glucocorticoid-induced bone loss and fragility in rats by orchestrating bone acquisition and resorption. Arthritis Rheum 65:1530–1540
24. Wei J, Shi Y, Zheng L, Zhou B, Inose H, Wang J, Guo XE, Grosschedl R, Karsenty G (2012) miR-34s inhibit osteoblast proliferation and differentiation in the mouse by targeting SATB2. J Cell Biol 197:509–521
25. Stahn C, Buttgereit F (2008) Genomic and nongenomic effects of glucocorticoids. Nat Clin Pract Rheumatol 4:525–533
26. Wei N, Yu Y, Joshi V, Schmidt T, Qian F, Salem AK, Stanford C, Hong L (2013) Glucocorticoid receptor antagonist and siRNA prevent senescence of human bone marrow mesenchymal stromal cells in vitro. Cell Tissue Res 354:461–470
27. De Iudicibus S, Lucafo M, Martelossi S, Pierobon C, Ventura A, Decorti G (2013) MicroRNAs as tools to predict glucocorticoid response in inflammatory bowel diseases. World J Gastroenterol 19:7947–7954
28. Honjo T (1996) The shortest path from the surface to the nucleus: RBP-J kappa/Su(H) transcription factor. Genes Cells 1:1–9
29. Bai S, Kopan R, Zou W, Hilton MJ, Ong CT, Long F, Ross FP, Teitelbaum SL (2008) NOTCH1 regulates osteoclastogenesis

directly in osteoclast precursors and indirectly via osteoblast lineage cells. J Biol Chem 283:6509–6518
30. Salie R, Kneissel M, Vukevic M, Zamurovic N, Kramer I, Evans G, Gerwin N, Mueller M, Kinzel B, Susa M (2010) Ubiquitous overexpression of Hey1 transcription factor leads to osteopenia and chondrocyte hypertrophy in bone. Bone 46:680–694
31. Deregowski V, Gazzerro E, Priest L, Rydziel S, Canalis E (2006) Notch 1 overexpression inhibits osteoblastogenesis by suppressing Wnt/beta-catenin but not bone morphogenetic protein signaling. J Biol Chem 281:6203–6210
32. Tezuka K, Yasuda M, Watanabe N, Morimura N, Kuroda K, Miyatani S, Hozumi N (2002) Stimulation of osteoblastic cell differentiation by Notch. J Bone Miner Res 17:231–239
33. Xu N, Liu H, Qu F, Fan J, Mao K, Yin Y, Liu J, Geng Z, Wang Y (2013) Hypoxia inhibits the differentiation of mesenchymal stem cells into osteoblasts by activation of Notch signaling. Exp Mol Pathol 94:33–39
34. Zhu F, Sweetwyne MT, Hankenson KD (2013) PKCdelta is required for Jagged-1 induction of human mesenchymal stem cell osteogenic differentiation. Stem Cells 31:1181–1192